Activation cross section measurement of the $^{100}Mo(\alpha,n)^{103}Ru$ reaction for optical potential studies

Journal of Physics: Conference Series **1668** (2020) 012041 doi:10.1088/1742-6596/1668/1/012041

Activation cross section measurement of the ^{100}Mo(α,n)^{103}Ru reaction for optical potential studies

T.N. Szegedi[1,2], G.G. Kiss[1], Gy. Gyürky[1] and P. Mohr[1,3]

[1]Institute for Nuclear Research, Bem square 18/c, H-4026 Debrecen, HU
[2]University of Debrecen, Egyetem ter 1, H-4032 Debrecen, HU
[3]Diakonie-Klinikum, D-74523 Schwäbisch Hall, Germany

E-mail: tn.szegedi@atomki.mta.hu

Abstract.

The light neutron-rich nuclei can be synthesized via (α,n) reactions in the so-called weak r-process. The abundances of these species are derived using reaction network calculations. Such a simulation has astrophysical and nuclear physics inputs, one of the most uncertain parameter is the α-nucleus optical potential. (α,n) cross section measurements can be used to evaluate α-optical potentials. For this purpose, the activation cross section measurement of the ^{100}Mo(α,n)^{103}Ru reaction is in progress at Atomki.

Keywords: nuclear astrophysics, activation method, weak r-process

1. Introduction

The synthesis of the heavy elements beyond iron is dominantly driven by neutron-capture reactions [1, 2]. However, the neutron-rich nuclei between ^{56}Fe and ^{109}Ag can be also synthesized in a neutrino-driven wind following the birth or merge of neutron stars in the weak r-process [3, 4]. This process runs close to the valley of stability and charged particle induced reactions — such as (α,xn), (α,γ), (p,xn) and (p,γ) — play important role in the production of light r-nuclei [5, 6, 7].

A widespread method to model this process is the use of reaction network calculations containing a few thousand reactions on almost a thousand, mainly radioactive nuclei. The network relies on astrophysical inputs — such as the temperature of the astrophysical site, the timescale of the process, the initial isotopic abundances etc. — and nuclear physics inputs like the reaction rates. Due to the lack of experimental data, the cross sections required to compute the reaction rates are calculated using the Hauser-Feshbach model (HF). The most uncertain input parameter of the HF model is the α-nucleus optical model potential (OMP). In many particular cases, the use of different α-OMPs can cause an order of magnitude difference in the predicted cross

Table 1. Decay properties of the reaction product taken from [11].

Target	^{100}Mo
Abundance	9.82±0.31 %
Product	^{103}Ru
Half-life	39.247±0.013 d [12]
γ-transitions	
E_γ	497.09 keV
I_γ	91.00±1.22 %

sections [5]. Therefore, the examination of the α-OMPs is necessary to strengthen the predictive power of the network calculations [6].

Often (α,n) cross section measurements are used to evaluate α-OMP's [6]. However, the existing data set regarding the weak r-process is scarce. The cross sections need to be measured at low energies where the predictions, calculated using different α-OMP's, are reasonably different. Such experiments are typically carried out using the activation technique. Unfortunately, (α,n) reactions on neutron rich isotopes often result in stable residual nuclei and therefore the activation technique cannot be used.

Furthermore, even if experimental (α,n) data exist, they are often contradictory. For instance, the ^{100}Mo(α,n)^{103}Ru cross section was measured in the 60's and 70's [8, 9]. There are differences in the experimental results, exceeding their uncertainties and moreover, the energy dependence of the measured points cannot be reproduced by theory [6]. By carrying out a new cross section measurement using thick molybdenum targets, a more precise database can be obtained and then this reaction can be used to evaluate the α-OMPs used in weak-r process calculations. Accordingly the activation cross section measurement of the ^{100}Mo(α,n)^{103}Ru reaction in the 7.9 MeV $\leq E_\alpha \leq$ 13.0 MeV energy range is in progress at Atomki using natural isotopic composition targets.

2. Experimental approach

2.1. Activity measurement

The activation method [10] was used to derive the ^{100}Mo(α,n)^{103}Ru cross sections. Thick molybdenum targets were irradiated with α-beam using the K=20 cyclotron accelerator of Atomki. The duration of the irradiation varied between 3 and 21 hours and the typical beam current was between 0.3 and 2 μA. The determination of the number of ^{103}Ru products was based on measuring the yield of emitted γ-radiation — after the irradiation — using a 50 % relative efficiency HPGe detector. The most important decay properties are presented in Table 1.

Two typical γ-spectra are shown in Figure 1. The E_γ = 497.1 keV and E_γ = 610.33 keV γ-peaks originate from the β-decay of ^{103}Ru. However, due to a background peak at

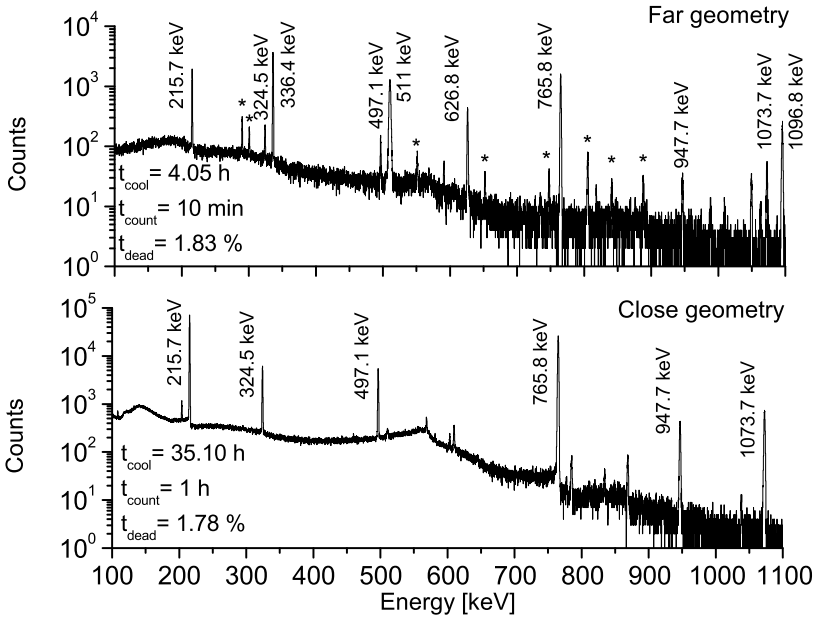

Figure 1. Typical γ-spectra. The relevant γ-transitions following the β-decay of the ^{95}Ru, ^{95}Tc, ^{97}Ru and ^{103}Ru isotopes are shown in black, blue, green and red colors, respectively. The stars represent the less intensive transitions belonging to the decay of ^{95}Ru.

$E_\gamma = 609.32$ keV (originating from the β-decay of ^{214}Bi) the $E_\gamma = 610.33$ keV γ-peak of ^{103}Ru was omitted from the analysis. The other transitions, shown in Figure 1, originate from the decay of ^{95,97}Ru.

2.2. Determination of the detection efficiency

In the investigated energy range the cross section spans four orders of magnitude. For the low energy irradiations high absolute detection efficiency is required, which can be achieved by reducing the detector-source distance. However, by going close to the detector surface the probability of the true coincidence summing increases. Moreover, the samples produced at higher energies would suffer from high dead time if the activity measurement were carried out in close geometry. Considering the above reasons, the cross section measurement was performed using two counting geometries: a larger sample-detector distance for the high energy irradiations ($E_\alpha \geq 10$ MeV) and a closer geometry to measure the low activities ($E_\alpha < 10$ MeV).

The absolute detection efficiency was measured at 21 cm detector endcap-source distance (far geometry) using the following calibration sources (activity uncertainty is given in parenthesis): ^{60}Co (1.5 %), ^{133}Ba (1.5 %), ^{137}Cs (1.5 %) and ^{152}Eu (2.0 %). The measured efficiency points were fitted with the following function [13],

$$\frac{1}{A \cdot {E_\gamma}^B + C \cdot {E_\gamma}^D} \tag{1}$$

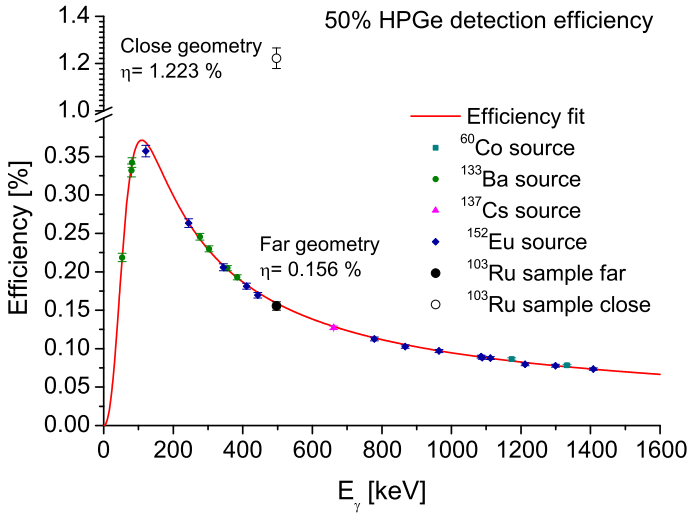

Figure 2. Absolute detection efficiency of the 50 % HPGe detector. The γ-transitions belonging to the calibration sources are shown in cyan (^{60}Co), green (^{133}Ba), pink (^{137}Cs) and blue (^{152}Eu). Furthermore, the efficiency of the $E_\gamma = 497.1$ keV transition is derived for both geometries.

where the A, B, C and D are the free parameters. The measured efficiency points and the fitted function are shown in Figure 2. According to the fitted curve, the efficiency at the $E_\gamma = 497.1$ keV ^{103}Ru transition is 0.156 ± 0.006 % in far geometry (black dot). The uncertainty of this point is defined by the quadratic sum of the activity uncertainty of the calibration sources (1.5 - 2.0 %), the relative intensity error of the calibration γ-transitions (<1.9 %), the statistical uncertainty of the measured points (0.1 - 1.0 %) and the error caused by fitting different functions to the points (2.0 %). Hence, the efficiency has 3.6 % relative uncertainty in far geometry.

To derive the detection efficiency at close geometry the following approach was used. Strong ruthenium sources — produced at $E_\alpha = 11.5$ MeV and $E_\alpha = 13.0$ MeV — were measured first in far geometry where the typical dead time was less than 1.0 %. When the sample activity decreased to a reasonable level, the sample was moved to 5 cm from the detector endcap (close geometry). By applying the decay law, the time difference between the two measurements can be taken into account and an efficiency correction factor between the two geometries can be obtained. The final efficiency correction factor for the $E_\gamma = 497.1$ keV γ-transition was derived from the weighted average of ratios derived from each irradiation. The detection efficiency in close geometry is 1.223 $\pm$ 0.045 % (black circle). As a conservative estimation we summed the uncertainty of the efficiency correction factor (0.2 %) and the far geometry efficiency error (3.6 %) and accordingly the close geometry efficiency has a 3.8 % relative uncertainty.

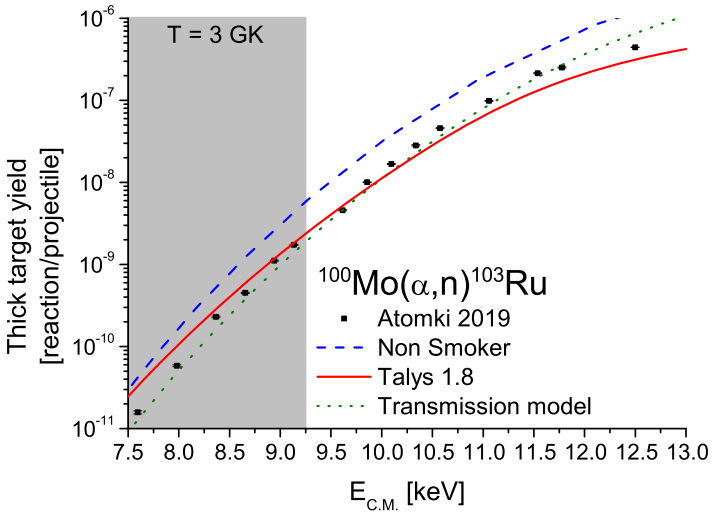

Figure 3. Preliminary ^{100}Mo(α,n)^{103}Ru thick target yield results compared to theoretical predictions calculated using the Talys 1.8 code (red line), Non Smoker code (blue dashed line) and a simple transmission model calculation (green dotted line).

3. Outlook

The detailed analysis of the ^{100}Mo(α,n)^{103}Ru reaction is in progress. The preliminary thick target yield results and their comparison to theoretical predictions using the default inputs of the Talys 1.8 [14] and Non Smoker [15] codes and the prediction of the barrier transmission model calculation [16] — further details see also P. Mohr *et al.* in these proceedings — are presented in Figure 3. Several points were measured in the Gamow-window (gray area). From the thick target yields, cross sections will be derived and compared to previous experimental data sets and theoretical predictions using different α-nucleus OMPs. Furthermore, a few more data points will be measured at lower energies.

Acknowledgments

This work was supported by NKFIH (K120666, NN128072). G.G. Kiss acknowledges support from János Bolyai research scholarship of MTA Atomki. This work was supported by the ÚNKP-18-4-DE-449 New National Excellence Program of the Ministry of Human Capacities of Hungary.

References

[1] F. Käppeler *et al.,* Rev. Mod. Phys. **83**, 157 (2011).
[2] F.K. Thielemann *et al.,* Annu. Rev. Nucl. Part. Sci. **67**, 253 (2017).
[3] S. E. Woosley, Astrophys. J. and R.D. Hoffman **395**, 202-239 (1992).

[4] Y.-Z. Qian and G.J. Wasserburg, Phys. Rep. **442**, 237268 (2007).
[5] J. Pereira and F. Montes, Phys. Rev. C **93**, 034611 (2016).
[6] J. Bliss *et al.,* J. Phys. G: Nucl. Part. Phys. **44**, 054003 (2017).
[7] P. Mohr, Phys. Rev. C **94**, 035801 (2016)
[8] R.A. Esterlund and B. D. Pate, Nucl. Phys. **69**, 401 - 422 (1965).
[9] H.P. Graf and H. Münzel, J. inorg. nucl. Chem. **36**, 3647 - 3657 (1974).
[10] Gy. Gyürky *et al.,* Eur. Phys. J. A **55**, 41 (2019).
[11] D. De Frenne, Nucl. Data Sheets **110**, 20812256 (2009).
[12] J.R. Goodwin *et al.,* Phys. Rev. C **80**, 045501 (2009).
[13] R.C. McFarland *et al.,* Radioact. Radiochem. **2**, 35 (1991).
[14] A.J. Koning *et al.,* AIP Conf. Proc. **769**, 1154 (2005)
[15] T. Rauscher and F.-K. Thielemann, At. Data Nucl. Data Tables **79**, 47 (2001). https://nucastro.org/nonsmoker.html
[16] P. Mohr, Int. J. Mod. Phys. E **28**, 1950029 (2019).